The Journal of Experimental Biology 200, 2705–2722 (1997)
Printed in Great Britain © The Company of Biologists Limited 1997
JEB0993

THE MECHANICS OF FLIGHT IN THE HAWKMOTH *MANDUCA SEXTA*

I. KINEMATICS OF HOVERING AND FORWARD FLIGHT

ALEXANDER P. WILLMOTT* AND CHARLES P. ELLINGTON
Department of Zoology, University of Cambridge, Downing Street, Cambridge CB2 3EJ, UK

Accepted 4 August 1997

Summary

High-speed videography was used to record sequences of individual hawkmoths in free flight over a range of speeds from hovering to 5 m s^{-1}. At each speed, three successive wingbeats were subjected to a detailed analysis of the body and wingtip kinematics and of the associated time course of wing rotation. Results are presented for one male and two female moths. The clearest kinematic trends accompanying increases in forward speed were an increase in stroke plane angle and a decrease in body angle. The latter may have resulted from a slight dorsal shift in the area swept by the wings as the supination position became less ventral with increasing speed. These trends were most pronounced between hovering and 3 m s^{-1}, and the changes were gradual; there was no distinct gait change of the kind observed in some vertebrate fliers.

The wing rotated as two functional sections: the hindwing and the portion of the forewing with which it is in contact, and the distal half of the forewing. The latter displayed greater fluctuation in the angle of rotation, especially at the lower speeds. As forward speed increased, the discrepancy between the rotation angles of the two halfstrokes, and of the two wing sections, became smaller. The downstroke wing torsion was set early in the halfstroke and then held constant during the translational phase.

Key words: flight, kinematics, wing rotation, hawkmoth, *Manduca sexta*.

Introduction

Detailed analyses of kinematics are central to an integrated understanding of animal flight. Data on how wing and body movements change with flight speed are not only of interest in their own right, they are also essential for aerodynamic modelling and for consideration of the aerodynamic mechanisms being employed. Kinematic gait changes in birds and bats have, for example, been linked to the transition from a vortex-ring gait at slow speeds to a continuous-vortex gait at high speeds (e.g. Norberg, 1990; Rayner, 1995; Tobalske and Dial, 1996).

The kinematics of forward insect flight are still poorly understood despite a long history of investigations of the wingtip path. High-speed cinematography of tethered insect flight, as pioneered by Magnan (1934) and Chadwick and Edgerton (1939), has been used for quantitative studies of a number of groups including the Diptera (e.g. Hollick, 1940; Nachtigall, 1966) and the Orthoptera (e.g. Weis-Fogh, 1956; Zarnack, 1972). Multiple-view filming has permitted very detailed three-dimensional analyses of the kinematics to be undertaken (e.g. Nachtigall, 1966).

The relationship between tethered and true free flight is, however, not known. Even where there is approximate balance in the vertical and horizontal forces, the realism of the flight depends upon the unknown influence of the body angle imposed by the experimenter, the motivational state of the insect and the constraints on its degrees of freedom of movement which are imposed by the tether. Few studies have sought to compare the kinematics of free and tethered flight, but tethering was found to reduce wingbeat frequency significantly in locusts (Baker *et al.* 1981; Kutsch and Stevenson, 1981) and Heteroptera (Betts, 1986). Clear differences have also been observed between the kinematics of free-flying (e.g. Ellington, 1984*b*; Ennos, 1989) and tethered (Miyan and Ewing, 1985) flies. In the absence of a more complete understanding of how tethered flight relates to free flight, any extrapolation from the former must be treated with some caution.

A number of recent studies have analysed the kinematics during free flight (e.g. Ellington, 1984*b*; Ennos, 1989; Dudley and DeVries, 1990; Dudley and Ellington, 1990*a*; Cooper, 1993; Wakeling and Ellington, 1997). Integrated studies of flight mechanics should include investigation of the motion of the longitudinal wing axis and of the accompanying wing torsion for individuals flying over as wide a range of speeds as

*Present address: Kawachi Millibioflight Project, Japan Science and Technology Corporation (JST), Park Building 3F, 4-7-6 Komaba, Meguro-ku, Tokyo 153, Japan (e-mail: sandy@kawachi.jst.go.jp).

possible. Ideally, these experiments would be undertaken in the field, but a pragmatic compromise at present is to record free-flight sequences obtained under controlled laboratory conditions (Dudley, 1992). Flight chambers can readily be used to obtain sequences of hovering and slow forward flight (e.g. Ellington, 1984*b*; Ennos, 1989), but a variable-speed wind tunnel must be employed to obtain forward flight at speeds selected by the experimenter (Tobalske and Dial, 1996). Birds can be trained, although not without some difficulty (e.g. Tobalske and Dial, 1996), to fly at constant speeds in such wind tunnels, but insects cannot. Instead, correctly oriented steady flight must be sought by exploiting an element of their flight behaviour, usually the optomotor response (David, 1978; Dudley, 1987; Dudley and Ellington, 1990*a*; Cooper, 1993).

The difficulty in predicting the exact location of free flight, and the consequent need for wider fields of view, has precluded the multiple-view filming used with tethered insects (e.g. Nachtigall, 1966). Stereogrammetric methods are not appropriate for three-dimensional reconstruction from single-view images, and a number of novel techniques for kinematic analysis have been developed. The most detailed and robust of these methods was derived by Ellington (1984*b*) and later modified for non-horizontal camera angles by Dudley and Ellington (1990*a*). Suitable techniques for angle-of-attack analysis of single-view images are evaluated in Willmott and Ellington (1997*a*).

The present study describes an investigation of wing and body kinematics during free flight of the hawkmoth *Manduca sexta* L. over a speed range from hovering to 5 m s^{-1}. No clear picture exists to date of the kinematic changes which accompany increases in insect flight speed, but systematic studies of individuals flying over a range of speeds (e.g. Dudley, 1987; Dudley and Ellington, 1990*a*; Cooper, 1993) have been more successful at identifying trends than those in which data have been pooled either within or across species (e.g. Dudley, 1990; Bunker, 1993). The former approach was followed for this study, with the ability of hawkmoths to feed 'on the wing' being exploited to obtain steady flight sequences for individual moths over the entire speed range. The results for three individuals – two females and one male – are presented and the relative importance of the various parameters in determining flight speed is discussed. The plasticity of the bumblebee wingbeat at any given speed was noted by Dudley and Ellington (1990*a*). Three successive wingbeats were, therefore, analysed in all the flight sequences in order to investigate the extent of beat-to-beat variation in the kinematic parameters. Such variation might be expected to be greater for hawkmoths, with their synchronous flight muscle, than in groups with asynchronous muscle.

The temporal and spanwise changes in angle of attack of the wing are also presented. The wings were modelled as a series of chordwise strips, and the orientation of the strips is described by the 'angle of rotation' about the longitudinal wing axis. These angles provide a detailed record of the three-dimensional shape of the wing which can readily be converted to the angles of incidence more relevant for use in aerodynamic analyses.

Materials and methods

Insects and filming

Manduca sexta were obtained as pupae from a population maintained at the Department of Zoology field station, Cambridge, UK. Filming took place in a room held at 23±2 °C. The experimental apparatus (Fig. 1A) consisted of a large L-shaped cage suspended around a streamlined feeder (Fig. 1B,C) positioned at the mouth of an open-jet wind tunnel. The cage was made from black nylon entomological netting, which provided good grip for the moths and transparency for the observer but which was soft enough to avoid excessive wear on the wing margins from contact with the sides. Small openings in the net allowed moths flying near the feeder to be filmed simultaneously from two cameras connected to a high-speed video system (see below).

The artificial flower (Fig. 1B) was designed to minimize the disruption to the airstream, whilst still providing a supply of nectar. The feeder was constructed around a length of 3 mm wide stainless-steel tubing which was slightly flattened parallel to the airflow, and which was attached *via* Tygon tubing to a 2 ml syringe from which the feeder could be refilled with honey-water (10 % by volume). A strip of black card (80 mm×40 mm) was wrapped around the steel tubing forming a streamlined, symmetrical aerofoil which was found, using the flow visualization techniques described in Willmott *et al.* (1997), to cause only very limited disruption to the airflow downstream. 'Petals' to aid location of the flower by the moths were made from brass shim oriented parallel to the flow. The shim and the top of the black card were painted white.

The open-jet wind tunnel used in this experiment was of a similar design to that used by Weis-Fogh (1956) and Dudley and Ellington (1990*a*), but with increased honeycombing of the main body to improve the airflow. The fan speed was controlled by a variac and monitored by measuring the frequency at which teeth on the drive cog passed an integrated infrared emitter/detector (RS 307913) whose output was fed into a Thandar TF200 frequency meter. The relationship between fan speed and air speed was determined each day using a Prosser AVM502 low-speed, bead thermistor anemometer. The anemometer was also used to measure the turbulence of the flow at 0.25, 1, 3, 4 and 5 m s^{-1}. Sampling at 21 points in the area within which the moths were filmed, the turbulence (the root mean square as a percentage of the mean velocity) was typically less than 1 %. There was a slight asymmetry in the turbulence with the highest values, exceptionally up to 4 %, in the lower half of the tunnel, below the region in which the moths were flying.

A Kodak EktaPro 1000 high-speed video system was used for all the filming, with the video output combined from two cameras fitted with Fujinon 12.5–80 mm TV zoom lenses. Camera A, placed behind and above the moth (Fig. 1A), provided the main image for wing motion analysis. Camera B

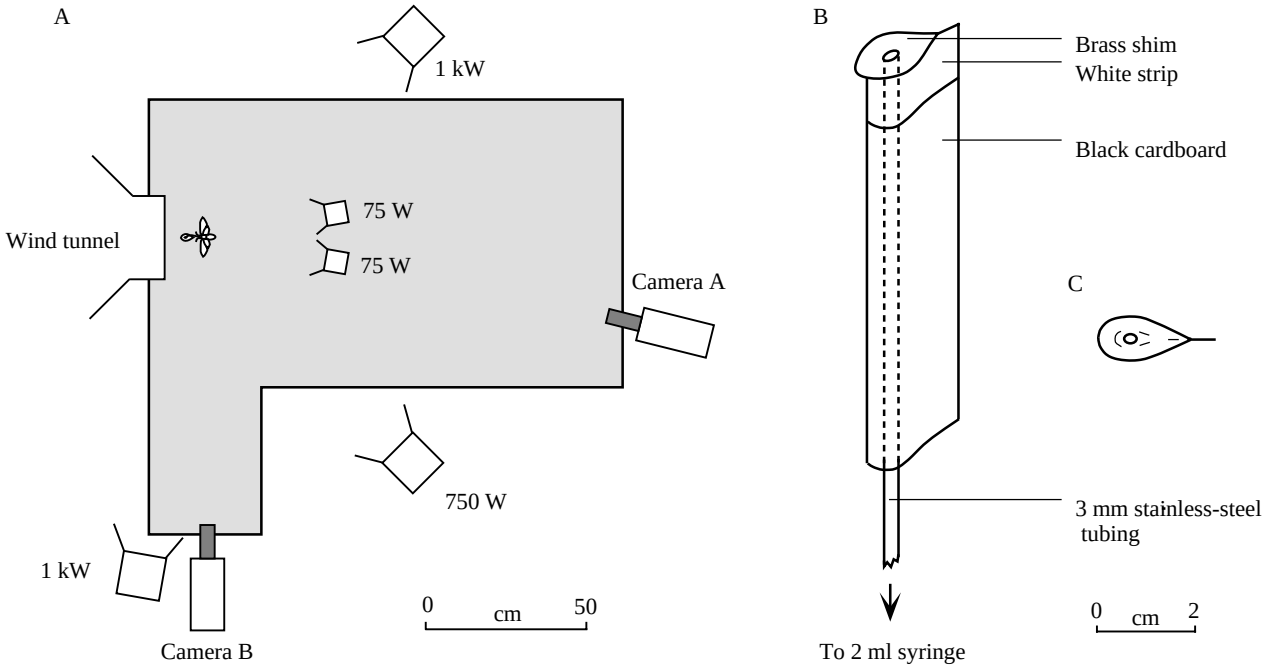

Fig. 1. The experimental apparatus used for filming. (A) Plan view showing the locations of the two cameras, and the locations and power ratings of the lights. A moth is shown in the desired position in front of the mouth of the wind tunnel. The shaded region indicates the area enclosed by the L-shaped flight cage. (B) An oblique side view of the feeder showing the cardboard aerofoil constructed around a central stainless-steel tube. (C) Top view of the brass shim which formed the 'petals' of the flower.

recorded a side view, showing the body orientation, which was superimposed onto the main view. The filming speed throughout was 1000 pictures s^{-1}, which is the fastest available for full-screen image recording. The EktaPro 1000 system has good low-light performance but, on account of the high filming speeds, a total of 2.9 kW of lighting was required to illuminate the whole wing adequately throughout the wingbeat. All of the lights were filtered using red photographic gel to minimize perception by the moths, whose vision is limited at the red end of the spectrum (Schwemer and Paulsen, 1973).

At the start of the dark period, the main filming lights were turned off but a 60 W red bulb provided indirect lighting for observation of the moth's activity. A single cold light source, placed above the exit of the tunnel, illuminated the feeder with white light to provide a strong stimulus for the foraging moths. When a moth was probing in or around the feeder, the filming lights were slowly brought up to full power (using a variac) to avoid disturbing the insect. At the same time, a VHS camera recording the EktaPro session number and time (from the EktaPro monitor) and the fan blade frequency (from the frequency meter display) was switched on and left running throughout the moth's period of activity. The moth was flown over the full range of speeds with, where possible, at least 4 s of flight (approximately 100 wingbeats) at each speed. Some moths lost interest in feeding at the higher speeds and so the protocol used was for the speeds to increase from 0 to 5 m s^{-1}. At 0 and 1 m s^{-1}, some moths were not oriented directly into the tunnel and a brief burst of air at a higher speed was required to correct this before the lower speeds were filmed. The feeder was refilled after the flights for a particular moth had been completed.

Morphology

Once a moth had finished flying, the filming lights were turned off and the moth was allowed to settle on the netting. After 15 min, the moth was sufficiently inactive to be captured and placed immediately, inside a plastic lunch box, into a freezer. One hour was long enough to kill the moth without any freezing of body water, leaving it in a flexible state. A range of body and wing morphometric measurements similar to those described in Ellington (1984*a*) were then determined; the results are given in a companion paper (Willmott and Ellington, 1997*b*). A video image of the right wing couple in flight position was converted into a wing outline, and the coordinates of the leading and trailing edges at 50 evenly spaced intervals along the length of the wing were determined using the NIH Image processing package (National Institutes of Health, Bethesda, MD, USA).

Wingtip and body kinematics

The flight sequences were downloaded from the EktaPro system to U-matic video format for analysis and storage. At each speed, three successive wingbeats were digitized from the period of steadiest flight. Each frame was grabbed onto a Macintosh Quadra 650 computer using a Neotech IG24 image acquisition board and stored as a TIFF file for subsequent

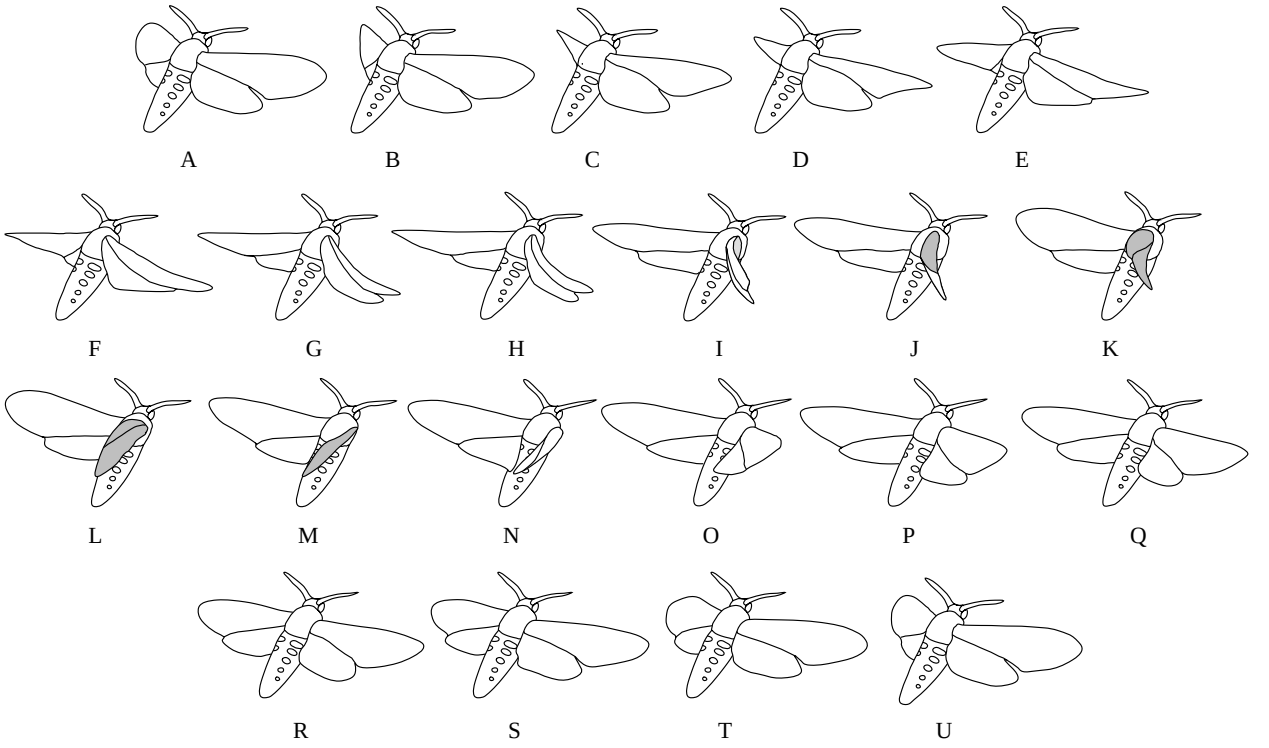

Fig. 2. *Manduca sexta* wing outlines traced from a high-speed video sequence of hovering flight. A complete wingstroke is shown, with frames A and U representing the mid-point of supination. The viewpoint is different from that used in the kinematic analysis: it provides a clearer picture of the motion and twisting of the near wing, but it is not so good for accurate digitization of the far wingtip and wingbase. Shaded areas indicate the ventral surface of the wing.

analysis. The coordinates of the near and far wingbase and wingtip in each individual frame were digitized using the NIH Image software package. The coordinates were translated to place the near wingbase at the origin, corresponding to the (x^*,y^*,z^*) coordinate system that is the starting point for the three-dimensional reconstruction of the wingbeat described by Ellington (1984*b*) and Dudley and Ellington (1990*a*). A program written in Mathematica (Wolfram Research, Inc., Champaign, IL, USA) was used to calculate the wingtip kinematic parameters given in the Symbols list.

The mean wingbeat frequency was determined from the period between the middle of supination at the start of the first wingbeat and the same point at the end of the third beat. A slight complication arose from the loss of every sixth frame during downloading from the EktaPro system to PAL format, but this did not affect the accuracy of the time clock displayed in each frame. The apparent body angle was measured from the side view image for every fourth frame. The mean angle for each beat was corrected for any observed yaw to give the true body angle.

The potential sources of error in the kinematic parameters, and estimates of their magnitude, are discussed in the Appendix.

Angle of rotation analysis

The middle wingbeat of each sequence was subjected to the Strips method for angle-of-attack analysis detailed in Willmott and Ellington (1997*a*). The wing outline was digitized from every second frame. The near wing was used wherever possible but in some frames at the top of the wingbeat, when the camera axis was close to the longitudinal axis of the wing, the near wing was greatly foreshortened and the far-wing outline was digitized instead.

The true outlines were compared with the predicted outlines of wing strips derived from the wing-shape analysis mentioned above. For the angle-of-rotation analysis, the 50 strips were amalgamated into 25 wider strips which were rotated individually about the longitudinal wing axis for each frame. The predicted outline was oriented using the appropriate sweep and elevation angles, and displayed with the true outline. The strips were rotated interactively until they coincided with the digitized outline. The angle through which each strip was rotated was defined as the ‘angle of rotation’ about the longitudinal axis. The angle of rotation is identical to the angle of attack relative to the stroke plane when the elevation angle is zero, but it differs somewhat for non-zero elevation angles. When the longitudinal wing axis lies outside the stroke plane, the angle of attack does not vary smoothly from 0 to 180 °; there is a discontinuity on either side of 90 °. For *Manduca sexta*, the wing axis may be depressed by as much as 25 °, and this effect is large. The angle of rotation, which is a linear measure of the orientation of the wing strips, is therefore preferable as a kinematic variable.

Angles of rotation were recorded at 0.1R intervals from 0.3R

to 0.9*R*, where *R* is the wing length. The area between the wingbase and 0.3*R* contains the anojugal region of the hindwing, which undergoes significant folding and consequent area changes during the course of a wingbeat. Many strips in this region proved impossible to match (Willmott and Ellington, 1997*a*), and the errors would have been unquantifiable.

Results

Flight behaviour and performance

Flight at low speeds (0–2 m s^{-1}) was characterized by long periods during which a very steady body position was maintained downstream of the feeder, interspersed by smooth manoeuvring. Control of flight presented no problems; steady flight was observed even with the body at appreciable yaw angles to the oncoming air. Plasticity of the kinematics could be seen clearly between different flight sequences at the same speed.

Long sequences of steady flight were less common at higher speeds as rolling and yawing motions became more pronounced. Continual slight adjustments were needed to correct the body position and large body yaw angles were not seen. The feeding motivation, however, remained high: even if the moths were displaced from their position as speed was increased, they rapidly returned to the feeder. The only exceptions were at 5 m s^{-1} when some of the moths were unable to fly steadily and thus abandoned their attempts to feed. Those moths that could fly at the highest speed often bobbed slightly up and down downstream of the feeder, accelerating slowly forwards and upwards for a few wingbeats before reducing their wingbeat amplitude (sometimes even appearing to glide momentarily) and falling back slightly.

Qualitative description of the wingbeat

A typical hovering wingbeat is shown in Fig. 2. At the bottom of the stroke (frame A), the wingtips are still widely separated when supination begins. Rotation proceeds about an axis close to the longitudinal axis of the wing, with the stiff leading edge supinating first (frames B–D). Torsion is almost simultaneous along most of the leading edge, which functions as a rigid spar, but the most distal quarter is more flexible and continues to translate ventrally for a short distance before rotating. The latter results in a slight ventral flexion of the longitudinal axis which is most marked in the distal region.

Rotation in the posterior regions of the wing appears to follow passively the torsion at the leading edge: the hindwing rotation lags behind that of the forewing, and the wing couple flexes slightly where the two wings meet (frames C,D). The time delay is most pronounced in the anojugal region whose inner edge is in contact with the side of the abdomen.

The trailing edge is still supinating as the leading edge begins the upstroke translational phase (frames E, F). The initial translatory movement is backwards, in a more horizontal path than the downstroke, and slightly in towards the body. This motion pushes the anojugal region against the body, causing it to fold along well-defined lines. As the upstroke proceeds (frames F–I), the wingtip slowly unflexes and the whole wing couple becomes more planar as the posterior areas also translate. The phase of the leading edge still precedes that of

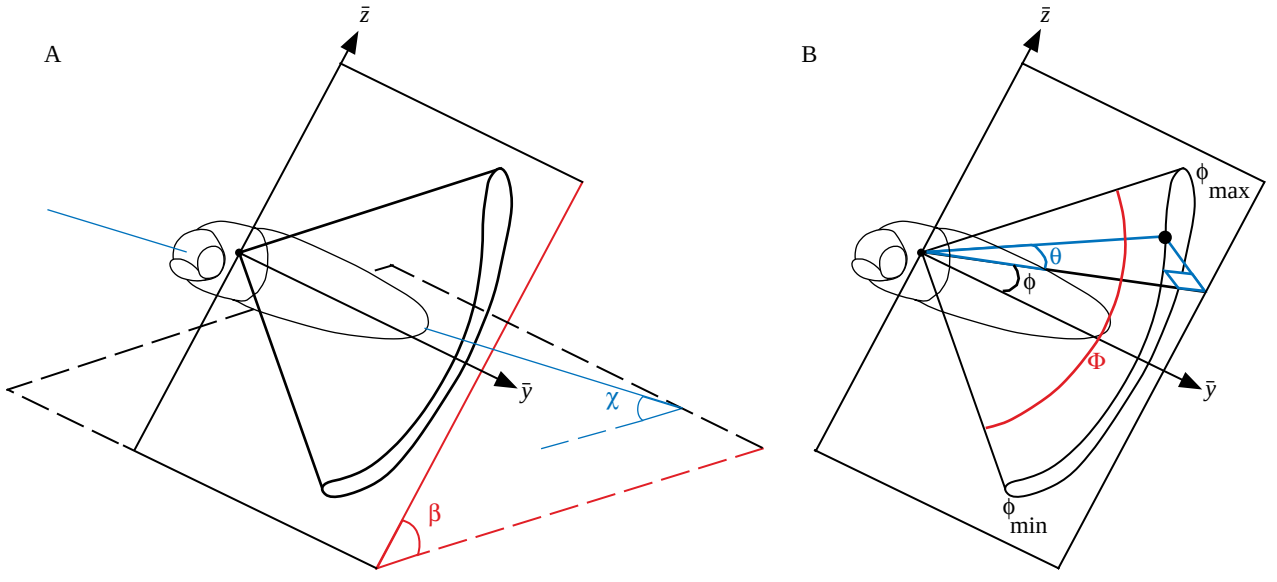

Fig. 3. Summary of the kinematic parameters calculated from the video sequences. (A) The stroke plane angle β and the body angle χ relative to horizontal. The stroke plane (the $\bar{y}\bar{z}$ plane as defined by Ellington, 1984*b*) is indicated by solid lines, a horizontal plane by broken lines. (B) Wing position parameters within the stroke plane. With the wingtip at the location indicated by the filled circle, the sweep angle ϕ is the angle between the $\bar{y}$ axis passing through the wingbases (Ellington, 1984*b*) and the projection of the longitudinal axis onto the stroke plane. The elevation angle θ is the angle between the wing axis and the stroke plane. The stroke amplitude Φ is the angle between the maximum and minimum sweep positions ϕ_{max} and ϕ_{min}, respectively.

the trailing edge, however. The rotation axis during pronation is again close to the longitudinal axis, but the extent of rotation is less pronounced than during supination. The longitudinal wing axis continues to move throughout pronation (frames K, L), in contrast to early supination where it is relatively still through several frames of the video sequence (frames A–D).

The posterior regions reach the top of their translation significantly later in the wingbeat, and the trailing edges of the hindwings come close to touching (frames M, N). At this stage, the anojugal flap is flat against the abdomen. During pronation, therefore, the forewing movements show a slight 'near peel' (Ellington, 1984*b*) with the left and right wings remaining well separated. The posterior regions perform a 'partial clap and peel' (Ellington, 1984*b*).

During the subsequent long translational phase of the downstroke (frames O–U), the wings are extended slightly as they move downwards, stretching the anojugal region of the hindwings and increasing the surface area of the wing couple. From early in this phase, there is little more camber in the wings than that inherent in the vein structure. This shape persists until the longitudinal axis once again reaches its minimum position, and supination begins.

Symmetry between the left and right wing couples was good; the marked asymmetry described by Weis-Fogh (1973) was seen only during manoeuvring. The coupling mechanism between the fore- and hindwings worked very effectively; the wings came apart only during violent and large-amplitude wing motions associated with abrupt manoeuvres (as in Weis-Fogh, 1973) and the coupling was restored during the next downstroke. Rapid turns and other high-lift manoeuvres resulted in the wings approaching more closely during pronation, with a full clap at the trailing edge of the hindwings.

The major elements of the wingbeat described above were observed at all speeds. Two trends were evident, however, as the speed increased. The first was that the wing became more rigid: the phase differences between wing regions decreased, resulting in less pronounced variation in rotation angle along the wing length. This change was particularly evident during supination, where the ventral flexion became very slight. The second trend was that the wingtip path moved posteriorly as speed increased; the folds in the anojugal region deepened and this region contributed little to the wing area.

Wingtip and body kinematics

Flight sequences were analysed for three moths: two females (F1 and F2) and one male (M1). The range of flight speeds V for each individual, along with the observed body roll and yaw angles (relative to horizontal and the tunnel axis, respectively), are given in Table 1. For forward flight, sequences were accepted only where the yaw angle was less than 10°. Roll angles were always less than 4° from horizontal. For moths M1 and F1, steady flight sequences were only obtained at five of the six desired speeds. The body mass m and forewing length R are given as indicators of the relative sizes of the moths; details of the wing and body morphology can be found in Willmott and Ellington (1997*b*).

Table 1 also includes the results of the detailed kinematic analyses. For each sequence, the parameter values are given for the individual wingbeats (denoted by letters A–C), along with the mean values over the three wingbeats. The wingtip and body parameter definitions are summarized schematically in Fig. 3; a detailed description is given in Ellington (1984*b*).

Stroke plane angle, body angle and wingbeat frequency

The relationship between forward speed and the stroke plane and body angles is shown in Fig. 4. The data points represent

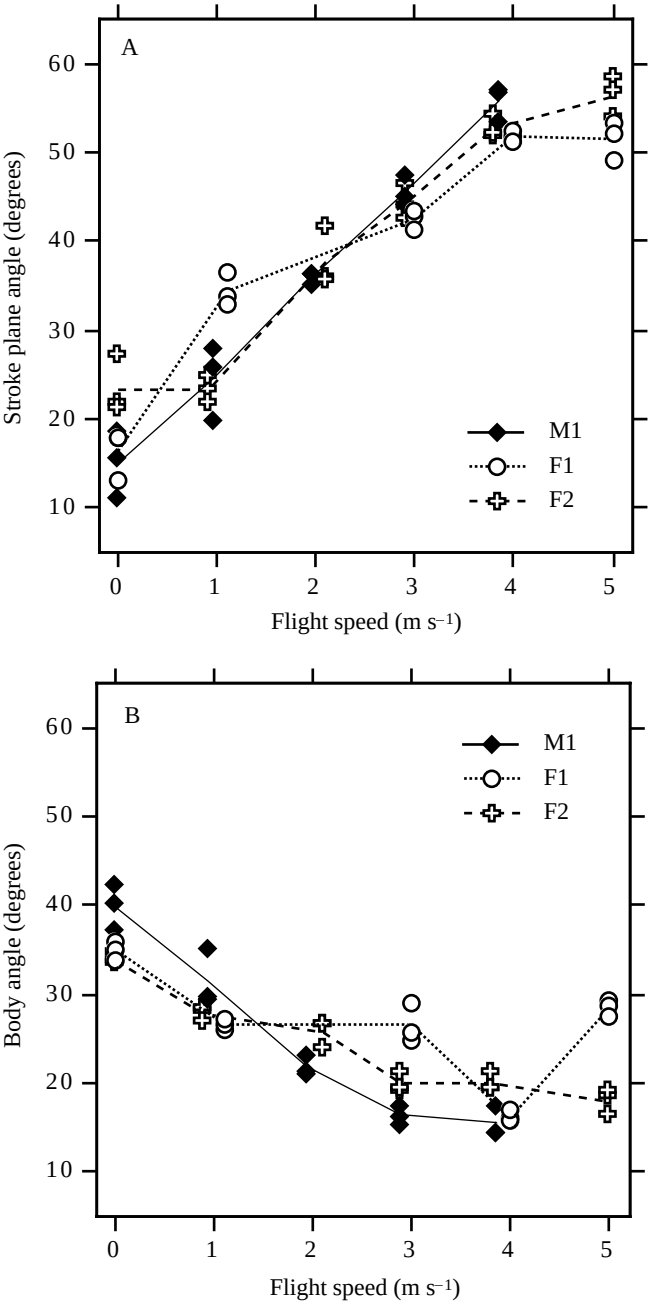

Fig. 4. The relationship between flight speed and (A) stroke plane angle and (B) body angle. Points represent the values for individual wingbeats; lines pass through the mean of the three wingbeats at each speed.

the values for individual beats; the lines are drawn through the mean values at each speed. The stroke plane angle β displayed a strong tendency to increase with speed from 10–30 ° at hovering to 50–60 ° at the highest speeds. The reverse trend was observed for the body angle χ, which was 30–40 ° at hovering but only 15–20 ° at 4 and 5 m s^{-1}. The body angle of 28.5 ° measured at 5 m s^{-1} for F1 was not characteristic of flight at this speed; the body angle was consistently lower during the less steady flight periods on either side of the selected sequence. There were small variations in the inclination of the body during the course of a wingbeat. The magnitude of these oscillations was typically 2–3 °, with the angles being highest during the downstroke. Most of this variation was due to movement of the whole body, but slight changes in the relative orientations of the thorax and abdomen were seen in some sequences.

The angle between the stroke plane and the longitudinal axis of the body was not constant: the nature of the wing articulation clearly permits changes in the orientation of the wingstroke relative to the body. In all three moths, the obtuse angle between the stroke plane and body axis [calculated as 180–(β+χ)] decreased from approximately 125 ° at hovering to approximately 105 ° at the highest speeds.

Wingbeat frequency *n* varied very little over the speed range (Fig. 5). With the exception of F1 at 4 m s^{-1}, all of the frequencies were within a narrow range between 24.8 and 26.5 Hz, with the variation for any individual being less than 1.5 Hz.

Wing positional angles and stroke amplitude

The changes with increasing speed in the amplitude and location of the wingstroke within the stroke plane are plotted in Fig. 6. The trend for stroke amplitude was for it to decrease from a maximum of approximately 115–120 ° at hovering to approximately 100–105 ° at the fastest speeds. The transition was not smooth: there was a marked decrease from hovering to 1 m s^{-1}, followed by a slower and less consistent decline between 1 and 5 m s^{-1}. For F2, the lowest amplitude (97 °) occurred at 3 m s^{-1}.

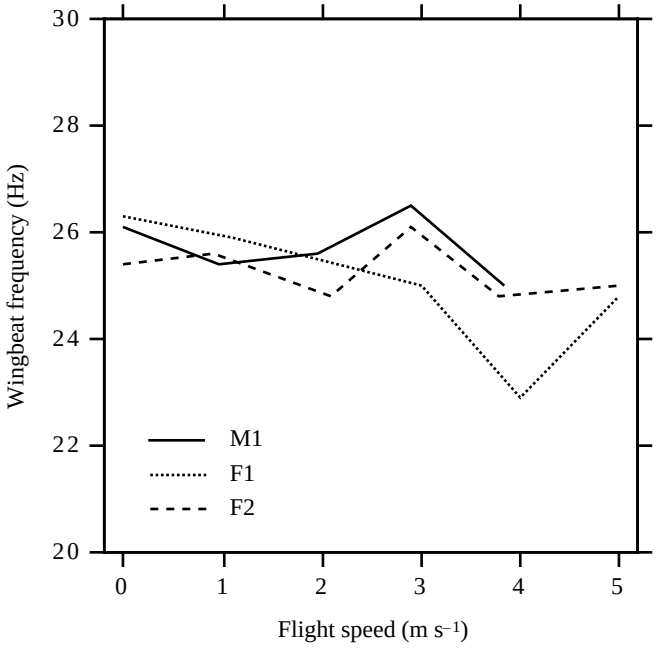

Fig. 5. The relationship between flight speed and wingbeat frequency. Values of frequency are averaged over the three wingbeats at each speed.

The reduction in amplitude resulted from changes in the position of supination. The minimum positional angle ϕ_{min} tended to become less ventral as speed increased from 0 to 2–3 m s^{-1}. For F2 and M1, the least negative ϕ_{min} (−25 to −30 °) occurred over this range, but for F1 it was not reached until 5 m s^{-1}. There were no clear trends in the maximum positional angle. For the females, the observed variation was very small: ϕ_{max} barely moved outside the range 70–75 °. Values for M1 exhibited greater scatter, but the mean values still varied by less than 7 °.

The dorsal movement in ϕ_{min}, combined with the constancy of ϕ_{max}, shifted the mean wing position $\bar{\phi}$ dorsally as speed increased. This change was concentrated between 0 and 3 m s^{-1}, over which interval the mean position moved by approximately 10 ° for all three moths. Above 3 m s^{-1}, there was little further change.

Wingtip paths

Fig. 7 illustrates the changes in wingtip path, as seen from a side view, for moth F2; similar trends were observed for the other two individuals. The origin of each graph is at the near wingbase, and all coordinates have been normalized to wing length. The body outline is drawn to scale and oriented at the correct angle to the horizontal.

During hovering, the wingtip path had an open-loop shape with the upstroke path lying posterior to that of the downstroke; the discrepancy was most marked in the top half of the stroke. The points were more clustered at supination than at pronation, supporting the earlier observation that the longitudinal axis was roughly stationary during much of supination. During pronation, the continuous, curved motion of the longitudinal axis spread the points out.

The paths at 1 m s^{-1} were generally similar to those at hovering, but as speed increased further two clear trends could be seen. First, the difference between the paths of the two halfstrokes decreased, resulting in a narrow, slightly J-shaped loop with a single cross-over. The qualitative difference between pronation and supination was also lost. Second, the entire wingbeat was moved ventrally and posteriorly relative to the wingbase. This can be seen in the changes in $\bar{\theta}$, the mean elevation or coning angle, which became more negative with increasing flight speed (Table 1). Fig. 7 also clearly illustrates the trends in stroke plane and body angles described above.

The time course of wingtip motion, as indicated by the positional angles ϕ and θ, and their variation with flight speed is shown for moth F2 in Fig. 8. The smoothed curves represent the first five terms of a Fourier series fitted to the data; the root mean square deviation (RMS, in degrees) between the data

Table 1. *The measured kinematic parameters from the analysed sequences*

V ($m\,s^{-1}$)	Wingbeat	Roll (degrees)	Yaw (degrees)	n (Hz)	β (degrees)	$\bar{\chi}$ (degrees)	Φ (degrees)	$\bar{\phi}$ (degrees)	ϕ_{min} (degrees)	ϕ_{max} (degrees)	$\bar{\theta}$ (degrees)
Moth M1 (m=1579 mg R=48.5 mm)											
	A				11.0	42.3	114.5	9.2	–48.0	66.4	–0.6
0	B				15.5	40.0	115.1	9.7	–47.9	67.3	–1.8
	C				18.5	37.2	113.5	8.8	–48.0	65.5	0.9
	Mean	0.8	4.1	26.1	15.0	39.8	114.4	9.2	–47.9	66.4	–0.5
	A				19.7	35.1	104.4	15.8	–36.5	68.0	–4.9
1.0	B				25.7	29.4	101.2	10.8	–39.8	61.4	–1.6
	C				27.7	29.5	111.5	15.2	–40.5	71.0	–2.5
	Mean	0.8	4.7	25.4	24.4	31.3	105.7	13.9	–38.9	66.8	–3.0
	A				36.1	22.9	110.6	18.8	–36.5	74.1	–8.7
2.0	B				36.3	21.0	109.4	15.7	–39.0	70.4	–8.0
	C				35.1	21.3	109.6	18.9	–35.9	73.7	–10.3
	Mean	1.4	2.0	25.6	35.8	21.7	109.9	17.8	–37.1	72.7	–9.0
	A				47.3	15.3	96.8	20.6	–27.8	69.0	–13.0
2.9	B				44.0	17.4	103.0	21.9	–29.6	73.4	–15.5
	C				44.8	16.2	100.4	20.7	–29.5	70.9	–14.1
	Mean	0.9	7.6	26.5	45.4	16.3	100.1	21.1	–29.0	71.1	–14.2
	A				53.4	17.3	99.7	18.3	–31.6	68.2	–15.8
3.9	B				56.8	14.4	99.4	18.0	–31.7	67.6	–16.0
	C				56.7	14.4	105.3	18.1	–34.6	70.8	–14.4
	Mean	3.7	4.7	25.0	55.6	15.4	101.5	18.1	–32.6	68.8	–15.4
Moth F1 (m=1648 mg R=51.9 mm)											
	A				17.8	35.8	121.9	10.8	–50.1	71.8	1.2
0	B				17.9	35.1	123.6	11.1	–50.7	72.9	1.2
	C				13.2	33.9	118.8	5.3	–54.2	64.7	–1.0
	Mean	2.2	16.8	26.3	16.3	34.9	121.4	9.1	–51.7	69.8	0.5
	A				33.8	25.9	108.1	17.3	–36.8	71.4	–9.0
1.1	B				33.0	26.5	106.4	18.0	–35.2	71.2	–10.6
	C				36.5	27.2	108.7	19.1	–35.3	73.5	–10.1
	Mean	1.8	2.5	25.9	34.4	26.5	107.7	18.1	–35.7	72.0	–9.9
	A				42.8	24.8	102.5	18.2	–33.1	69.4	–17.0
3.0	B				43.5	25.8	105.1	19.3	–33.3	71.8	–17.4
	C				41.4	29.0	110.3	18.8	–36.3	74.0	–14.6
	Mean	2.5	0.3	25.0	42.6	26.5	106.0	18.8	–34.2	71.7	–16.3
	A				51.9	16.1	99.4	22.1	–27.6	71.7	–20.5
4.0	B				52.3	15.7	103.5	21.6	–30.2	73.3	–19.8
	C				51.3	16.9	99.4	22.0	–27.7	71.7	–21.0
	Mean	3.4	7.4	22.9	51.8	16.2	100.8	21.9	–28.5	72.3	–20.4
	A				49.2	29.3	98.8	23.5	–25.9	72.9	–24.0
5.0	B				53.2	28.7	100.9	21.2	–29.2	71.6	–23.8
	C				52.0	27.5	99.8	22.8	–27.1	72.7	–22.5
	Mean	0.8	8.1	24.8	51.5	28.5	99.8	22.5	–27.4	72.4	–23.4

Table 1. *Continued*

V ($m\,s^{-1}$)	Wingbeat	Roll (degrees)	Yaw (degrees)	n (Hz)	β (degrees)	$\bar{\chi}$ (degrees)	Φ (degrees)	$\bar{\phi}$ (degrees)	ϕ_{min} (degrees)	ϕ_{max} (degrees)	$\bar{\theta}$ (degrees)
Moth F2 (m=1995 mg R=52.1 mm)											
	A				21.8	33.8	106.5	11.9	–41.3	65.1	2.2
0	B				21.1	34.6	115.7	18.6	–39.2	76.4	2.5
	C				27.2	33.4	117.4	17.2	–41.5	75.8	–2.1
	Mean	1.0	8.1	25.4	23.4	33.9	113.2	15.9	–40.7	72.4	0.9
	A				23.3	28.1	105.8	17.2	–35.7	70.1	–1.5
0.9	B				21.9	28.4	107.3	18.0	–35.7	71.6	–3.3
	C				24.7	27.0	103.4	16.2	–35.5	68.0	–4.0
	Mean	0.5	9.6	25.6	23.3	27.8	105.5	17.1	–35.6	69.9	–2.9
	A				35.8	26.7	98.5	23.2	–26.1	72.4	–6.3
2.1	B				35.5	26.7	100.2	24.5	–25.7	74.6	–6.6
	C				41.5	24.0	99.9	25.4	–24.5	75.3	–8.2
	Mean	3.5	4.9	24.8	37.6	25.8	99.5	24.4	–25.4	74.1	–7.0
	A				46.5	19.1	90.6	21.9	–23.4	67.2	–12.2
2.9	B				42.6	21.1	96.6	21.8	–26.5	70.1	–10.5
	C				44.0	19.5	104.1	20.7	–31.3	72.8	–8.4
	Mean	1.6	7.4	26.1	44.4	19.9	97.1	21.5	–27.1	70.0	–10.3
	A				51.7	19.3	102.8	22.0	–29.4	73.4	–10.8
3.8	B				52.1	19.5	102.2	22.0	–29.1	73.1	–13.0
	C				54.2	21.3	103.1	21.3	–30.3	72.8	–13.3
	Mean	1.0	2.2	24.8	52.7	20.0	102.7	21.8	–29.6	73.1	–12.4
	A				54.0	18.4	105.0	21.9	–30.5	74.4	–11.4
5.0	B				58.3	16.3	102.9	21.4	–30.1	72.8	–14.8
	C				57.0	19.2	103.7	21.2	–30.6	73.1	–15.1
	Mean	0.8	0.1	25.0	56.4	18.0	103.9	21.5	–30.4	73.4	–13.7

Mean values are given for roll and yaw angles, and for wingbeat frequency.

Data for the detailed wingtip parameters are presented for the three individual wingbeats (A–C) at each speed and for the mean of the three beats.

See the Symbols list and Fig. 3 for definitions of the parameters.

V, flight velocity.

points and the fitted curve is given as an indicator of the goodness of fit. The ratio of the downstroke duration to the upstroke duration (d/u, as determined from the timing of the maximum and minimum sweep angles in the raw data) is shown at the bottom of each graph.

The variation in sweep angle ϕ did not follow simple harmonic motion. The shape of the graphs is not only saw-toothed, but it also displays a marked asymmetry between the duration of the two halfstrokes. The downstroke duration as a proportion of the whole beat ranged from 0.51 to 0.67, with a mean value of 0.59 for the 48 wingbeats analysed in this study. The means for moths M1, F1 and F2 were 0.57, 0.59 and 0.60, respectively. There was no consistent trend between downstroke duration and forward speed; for M1 and F1, the duration tended to increase with increasing speed, but the opposite trend was recorded for F2. It should be noted that the relatively limited number of points per wingbeat meant that the temporal resolution of the analysis was not high. However, even making allowance for the potential errors discussed in the Appendix, the downstroke was consistently longer in duration than the upstroke.

The maximum projected wing length was always found in the downstroke; the ventral flexion seen during the early stages of the upstroke resulted in shortening of the projected wing length by approximately 1–2 % during these frames. The same effect was also responsible for the sudden jumps in sweep angle between upstroke points either side of the maximum projected length position which can be seen for ϕ near −10 ° in several of the graphs.

Angles of rotation

Figs 9 and 10 show the angles of rotation relative to the stroke plane α_{sp}. Fig. 9 presents the changes in α_{sp} for each strip from 0.3R to 0.9R during the course of the wingbeat with the most complete data set. It clearly demonstrates the functional division of the wing into two sections with regard

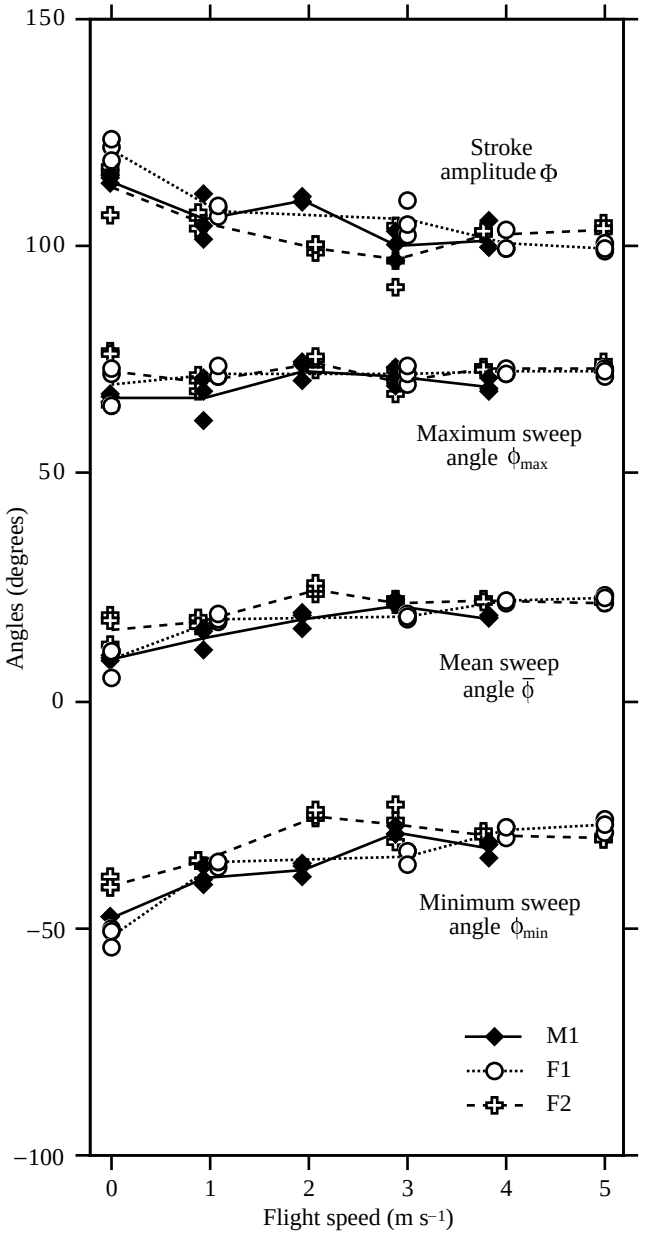

Fig. 6. The changes with increasing flight speed in the stroke amplitude and in the maximum, minimum and mean sweep angles which describe the location of the wingbeat within the stroke plane. Points represent the values for individual wingbeats; lines pass through the mean of the three wingbeats at each speed.

to the magnitude of the angles and the timing of major rotations. These two regions correspond to the hindwing together with the portion of the forewing with which it is in contact (strips 0.3*R* to 0.5*R*), and the more distal area of the forewing (0.6*R* to 0.9*R*). The variation in angle within each section is small and, for clarity, only the mean angle in each of the two sections is plotted in Fig. 10. The values for 0.9*R* were not included in the calculation of the mean values for the outer section; the chord at that point was so narrow that the measured angles were more susceptible to digitizing errors.

Fig. 10 contains selected graphs which illustrate how the changes in rotational angles varied with flight speed. The results are presented for hovering, for the fastest speed and for one intermediate speed for moths F2 and M1; in some other sequences, the upstroke data were incomplete owing to the problems discussed in Willmott and Ellington (1997*a*). The mean rotational angles for each of the two wing sections are shown, along with the time at which the wing is at its maximum and minimum sweep angles. The graphs indicate a consistent pattern for the changes in orientation during the course of the wingbeat: the most extreme values occurred during the translational phases, with the rotation between these values being concentrated into short periods around the end of each halfstroke. The highest angles were seen as a fairly sharp peak in the middle of the upstroke. The downstroke trough was more flattened: the minimum value was reached early in the downstroke and this orientation was held fairly constant throughout most of the subsequent translation.

There were, however, quantitative differences in these changes, both between the two wing sections and among different forward speeds. The outer half of the wing underwent more pronounced variation in its orientation than the inner half and hence rotated at higher angular velocities during the stroke reversals. The mean velocities during these periods were as high as $10\,000\,^\circ\,s^{-1}$ for the outer section, while the inner section seldom rotated at velocities higher than $5000\,^\circ\,s^{-1}$. These values should only be taken as rough estimates, but the difference between the two sections is clear.

The most extreme rotation angles and the most pronounced twisting along the wing were observed during hovering. During the upstroke, there was a difference of 20° or more between the angle of the outer wing section, which peaked at over 150°, and the angle of the inner section. The wing pronated rapidly at the top of the stroke, and a relatively sharp trough of rotation angle was reached early in the downstroke with the outer section at an angle of 35–45° and the inner section at approximately 5–10° steeper. Significant twisting along the length of the wing reappeared later in the translational phase as the inner section started to rotate in advance of the outer section.

A number of changes accompanied increases in flight speed: the range of rotation angles and the degree of twist along the wing became reduced, and the downstroke trough became more flattened, lacking the early minimum value seen during hovering. The rotation angles in both sections remained within the narrower range of 60–120° at the highest speeds.

Discussion

The kinematics of *Manduca sexta* hovering flight was cited by Weis-Fogh (1973) as being typical of ‘normal hovering’, a flight mode characteristic of many insects in which the stroke plane is approximately horizontal and in which the two halfstrokes make similar contributions to the lift. Whilst the observed asymmetries in the stroke mean that *Manduca sexta* may not be as representative as Weis-Fogh (1973) suggested,

there are a number of reasons why it is still a good species to use as a model for the changes in flight kinematics which accompany changes in forward speed.

First, the wingbeat kinematics contain the major elements which have been consistently identified in other insect species, but without any of the marked idiosyncrasies which have been seen in certain groups. *Manduca sexta*, for example, displays long periods of translation during which the wing orientation is relatively constant, separated by rapid rotation about an axis close to the leading edge. The stroke amplitude is close to the value of 120 ° that is often cited as typical for insects (e.g. Weis-Fogh, 1973), and a positive mean sweep angle indicates that the

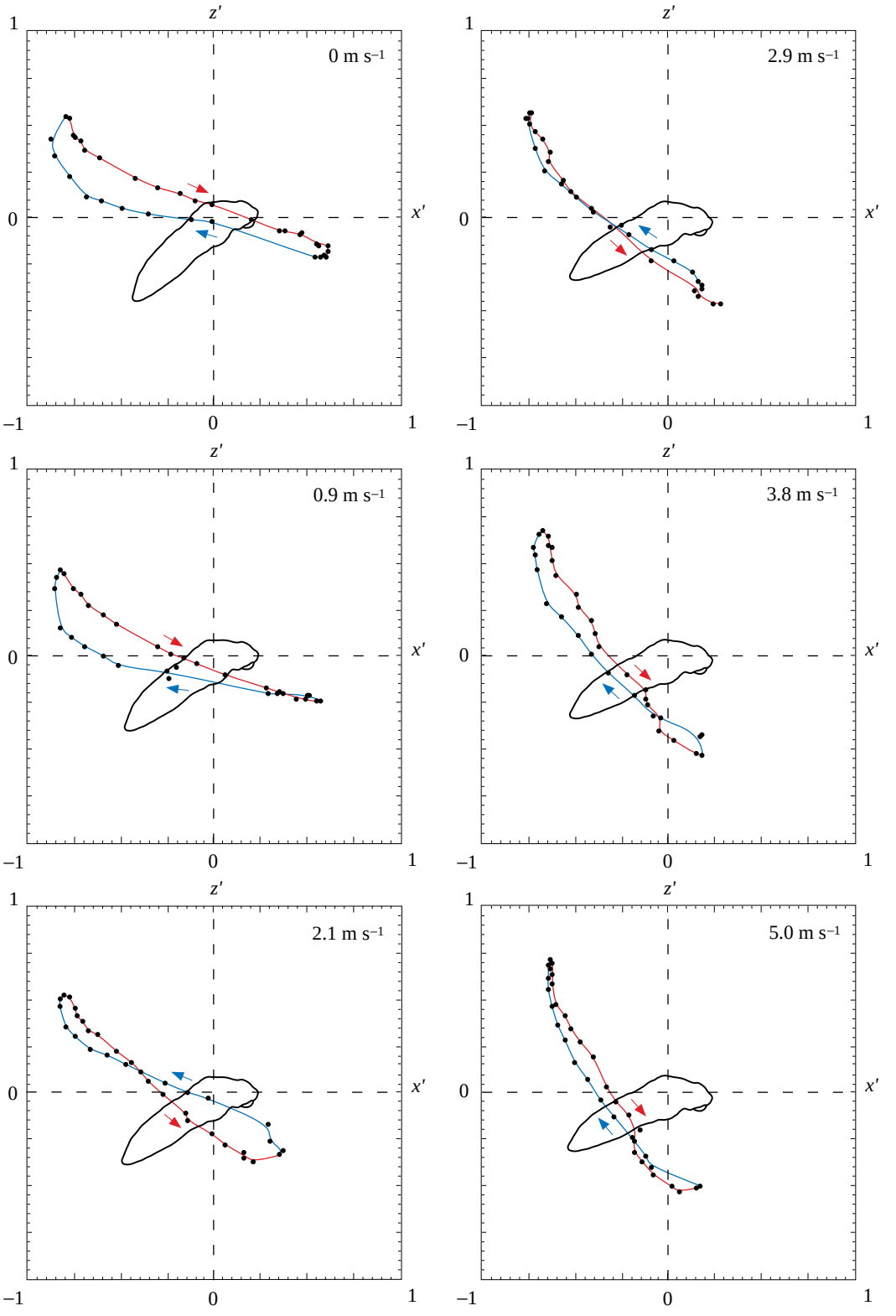

Fig. 7. Side views of the wingtip paths relative to the wingbase for moth F2 at the six different speeds. The downstroke paths are plotted in red, the upstroke paths in blue. The coordinate system is the body-fixed x',y',z' system defined by Ellington (1984*b*); the axes are normalized to wing length. In each graph, the body is inclined at the correct angle to horizontal.

left and right wings are closer together at pronation than at supination. The kinematics is not complicated by the full clap and peel seen in some butterflies (Betts and Wootton, 1988; Brodsky, 1991; Bunker, 1993), by the exaggerated ventral flexion observed in some Diptera (Nachtigall, 1979; Ennos, 1989) or by the Z-shaped wing deformations which have been noted for locusts (Jensen, 1956). The hawkmoth, therefore, offers a reasonably generalized wingbeat.

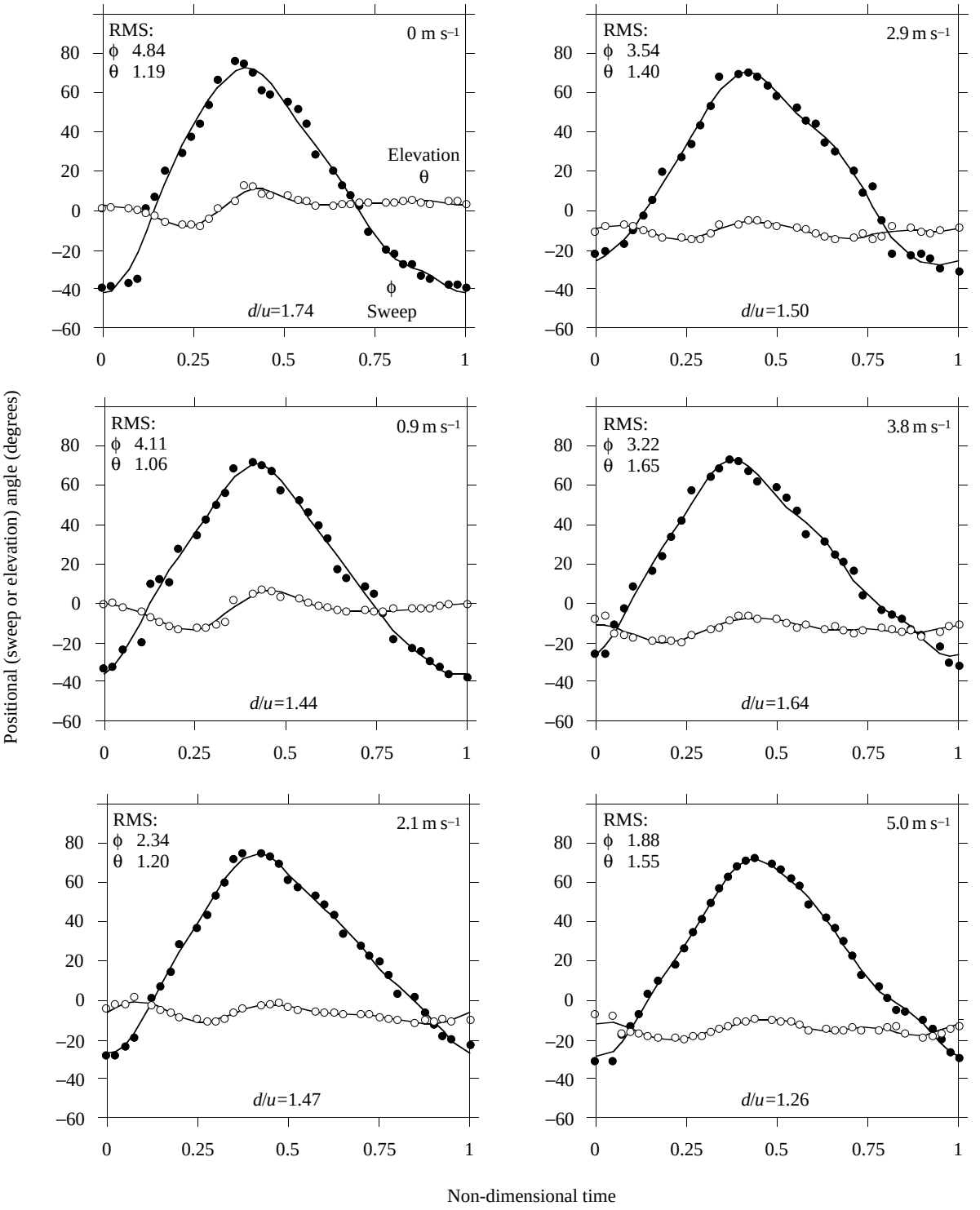

Fig. 8. The changes in sweep angle φ (filled circles) and elevation angle θ (open circles) during the course of wingbeats at different flight speeds for moth F2. Non-dimensional times of 0 and 1 represent the middle of supination when the wing is at its lowest position. Fitted lines are the first five terms of a Fourier series. See the text for further details. *d*/*u*, ratio of downstroke to upstroke duration; RMS, root mean square deviation (in degrees) between the data points and the fitted curve.

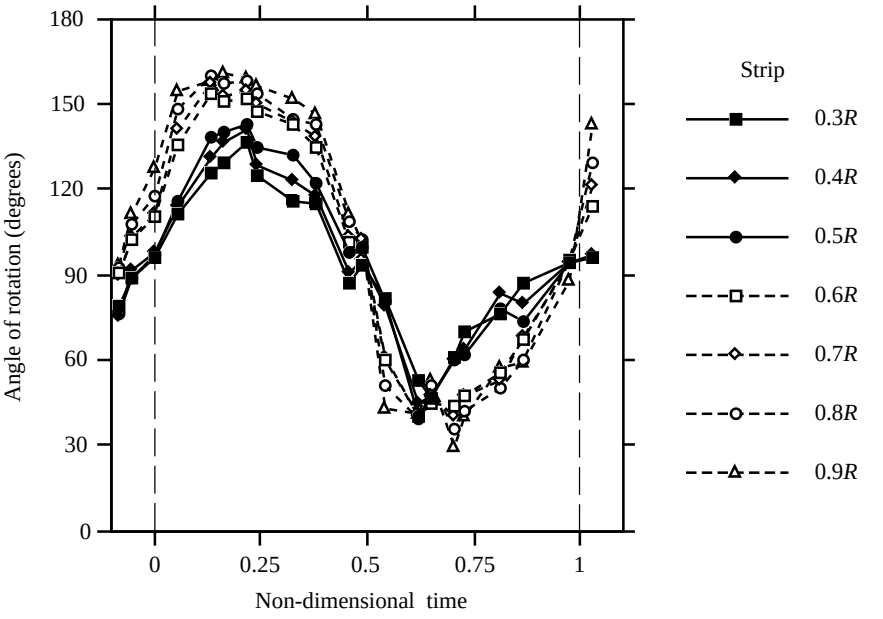

Fig. 9. A typical graph of the changes in angle of rotation α_{sp} for individual wing strips during the course of a wingbeat. These data are from moth M1 at $0\,m\,s^{-1}$. The stroke starts and finishes at mid-supination, the timing of which is indicated by the vertical dashed lines. The individual strips are coded according to whether they fall within the functional outer (broken lines, open symbols) or inner (solid lines, filled symbols) sections of the wing. *R*, wing length.

Second, the *Manduca sexta* wingbeat proved to be remarkably consistent. Significant intraspecific variation has been reported for many insect groups including butterflies (Betts and Wootton, 1988; Bunker, 1993) and flies (Ennos, 1989). However, the variation in kinematics between successive wingbeats, and also between individuals, was small in the current study. This simplified the task of separating the influence of flight speed on kinematic parameters from the noise of natural variation.

Changes in wingtip and body kinematics with forward speed

Manduca sexta displayed no clear 'gait' change with speed. Instead, there was a gradual change in the wingbeat between hovering and fast forward speeds. It is probably not helpful to dwell on details of the changes in the wingtip path since they are highly variable and reflect the indirect influence of many factors including control mechanisms at the wingbase and aerodynamic forces (Ellington, 1984*b*). The trends in the quantifiable parameters such as the stroke plane, body and wingtip positional angles prove more informative.

The clearest relationships observed in this study were that increases in forward speed tended to be accompanied by an increase in stroke plane angle and a decrease in body angle. These two angles are not independent; although some variation in the angle between the stroke plane and body axis was seen for *Manduca sexta*, the nature of the wing articulation forces these two parameters to change in tandem. Changing the stroke plane angle enables the direction of the resultant force to be altered: as the stroke plane becomes more vertical, the resultant is tilted forward in a manner that is similar to, but more complicated than, the control of flight in helicopters. The concomitant decrease in body angle with increased flight speed will reduce the parasite drag.

A similar relationship between speed and stroke plane and body angles was seen in the bumblebee *Bombus terrestris* (Dudley and Ellington, 1990*a*; Cooper, 1993), the hoverfly *Eristalis tenax* (Dudley, 1987) and, using pooled data from a number of individuals, in the moth *Urania fulgens* (Dudley and DeVries, 1990). The angle between the stroke plane and the body axis was more constant for these species, varying by less than 10° for the bumblebee and 5° for the hoverfly. The evidence from studies of butterflies is less clear cut. Betts and Wootton (1988) and Bunker (1993) found considerable variation in stroke plane and body angles for a range of papilionid and hesperiid species, but both studies noted that stroke planes tended to become more vertical at higher speeds.

Several studies of dipteran flight have found a significant relationship between flight speed and either stroke plane or body angle. David (1978) found an inverse correlation between speed and body angle in *Drosophila hydei* and concluded that the stroke plane angle controlled the resultant force, as it did in *Drosophila melanogaster* (Götz, 1968). Ennos (1989), however, found that freely manoeuvring flies could tilt their force vector by varying the relative lift of the two halfstrokes without having to change the stroke plane. He proposed that the force vector can be tilted more rapidly where its control is independent of the body angle. Once steady flight conditions have been reached, the body angle can then be changed to reduce the energetic cost of flight.

The link between flight speed and stroke amplitude is less clear. The animal flight literature does not support any particular relationship between these parameters (Dudley, 1987), but in studies where there was a trend it has generally been that amplitude decreased with increasing speed. A decrease was observed in tethered dragonflies (Gewecke, 1970) and locusts (Gewecke *et al.* 1974), and for free-flying bumblebees by Cooper (1993). Hollick (1940) found that the stroke amplitude of tethered *Muscina stabulans* decreased with

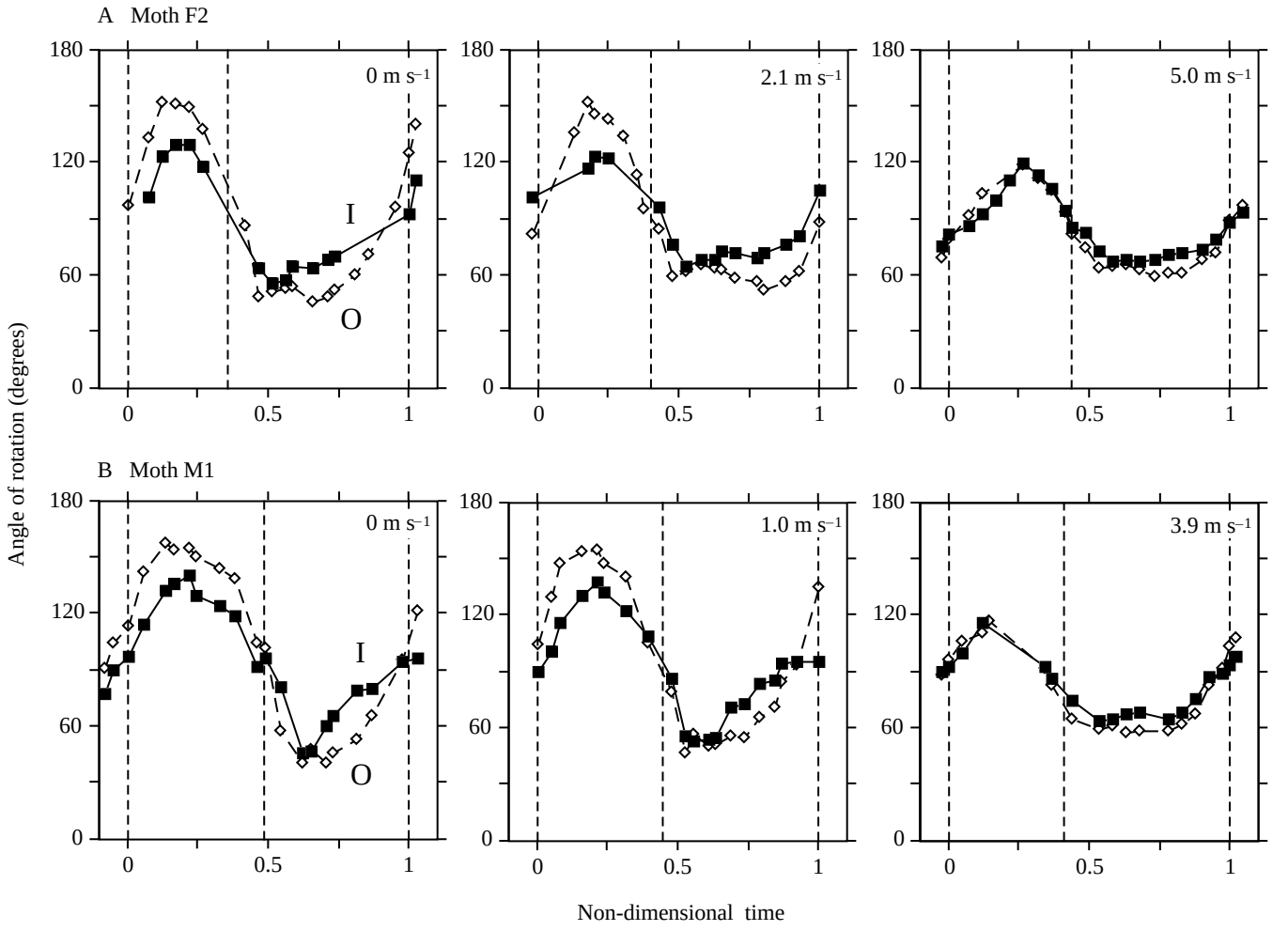

Fig. 10. Selected sequences from moths F2 and M1 which illustrate the changes in the pattern of rotation angle variation with increasing flight speed. The angles for the individual strips have been grouped into the mean angles for the inner (I; solid lines, filled squares) and outer (O; broken lines, open diamonds) functional wing sections. The outer two vertical dashed lines indicate mid-supination; the middle dashed line marks the time of mid-pronation.

increased speed and with lower body angles, and similar interdependence between the stroke plane angle and amplitude was noted by Vogel (1967) for *Drosophila virilis*. No significant relationship was found, however, between speed and stroke amplitude in hoverflies (Dudley, 1987), bumblebees (Dudley and Ellington, 1990*a*) or Lepidoptera (Dudley and DeVries, 1990; Bunker, 1993). This result is perhaps not surprising for butterflies where substantial variations in stroke amplitude are common: the range in Bunker's (1993) study was 23–181 °! Slow flight in some papilionids was characterized by large stroke amplitudes (Betts and Wootton, 1988).

The results for *Manduca sexta* provide strong support for a decrease in stroke amplitude with increasing flight speed, at least over the range from 0 to 3 m s^{-1}. Further increases in speed were not always accompanied by a further reduction in amplitude. The manner in which the amplitude is reduced may be as important as the magnitude of the reduction. For the hawkmoth, stroke amplitude is controlled through the minimum wing position: the separation between the wing couples during pronation was held constant, but the supination position became less ventral with increased flight speed. In combination, these trends caused a dorsal shift in the area swept by the wings, as indicated by an increase in mean wing position with increasing speed. This dorsal shift helps to produce the nose-down pitching moments (Ellington, 1984*b*) that are required to decrease the body angle as speed increases and it also counteracts the reduction in these moments which should result from the increase in stroke plane angle (Dudley and Ellington, 1990*b*). The necessary changes in mean sweep angle are small: Dudley (1987) estimated that for bumblebees the increase would only have to be 5–8 ° over a speed range of 0–4.5 m s^{-1}.

Comparative data for the changes in positional angles with speed are limited. Dudley and Ellington (1990*a*) described a similar increase in mean positional angle, resulting from variation in minimum positional angle, in bumblebees. Cooper (1993), however, found that the reduction in stroke amplitude

with increasing speed for the same species was due as much to a reduction in maximum wing position as to a change in minimum position. Overall, there was no significant change in mean wing position with speed.

Wingbeat frequency is comparatively easy to determine and it has long been studied in a wide range of insect groups. Sotavalta (1947, 1952, 1954) reviewed the early data on 'flight tone' which had either been determined from chronophotographic techniques (e.g. Magnan, 1934) or from his own extensive use of acoustic methods. His main purpose was to determine whether frequency was determined by wing inertia or air resistance (he concluded that the former was correct), but flight speed was one of a number of other influences which he considered. Schnell-Larsen (1934, cited in Hocking, 1953) reported that frequency in *Apis* sp. was a decreasing function of flight speed, but Sotavalta (1947) concluded that the opposite trend was, in general, true. However, he acknowledged some methodological problems and recognised that 'subsequent investigations may throw more light on the subject'.

These subsequent investigations have found no general relationship between flight speed and wingbeat frequency. A positive correlation was found in both free-flying (Baker *et al.* 1981) and tethered (Gewecke, 1975) locusts, but there was no relationship in free-flying individuals of any of the following groups: hoverflies (Dudley, 1987), moths (Dudley and DeVries, 1990) or bumblebees (Dudley and Ellington, 1990*a*). Bunker (1993) found that frequency increased with non-dimensional velocity across a range of butterfly species, but there were no trends in the data for individual species. Cooper (1993) obtained frequency measurements from a much greater range of speeds for individual bumblebees. She found that although frequencies for any particular individual never varied by more than 15 % there was a clear U-shaped relationship between speed and wingbeat frequency, with the lowest frequencies at intermediate speeds.

The data for *Manduca sexta* fit the general picture of a wingbeat frequency which is independent of flight speed. There was a tendency for frequency to decrease slightly with increasing speed but, with the exception of the value of 22.9 Hz for F1 at 4 m s^{-1}, all of the observed frequencies for the three moths fell within the narrow range of 24.8–26.5 Hz.

A restricted range of wingbeat frequencies would be expected for groups with asynchronous flight muscle such as Diptera and Hymenoptera. The flight musculature must function at the natural resonant frequency of the mechanical system involving the thorax and wings. The wingbeat frequency can be varied slightly to modulate power output, as seen in the slightly increased wingbeat frequency of loaded or fast-flying bumblebees (Cooper, 1993), by using accessory muscles to modify the thoracic properties (Nachtigall and Wilson, 1967; Josephson, 1981). These variations, however, are small. The same constraint on frequency does not apply to groups with synchronous flight muscle, but their musculature still appears to be working within a narrow range of physiological conditions. For the first dorsoventral muscle of *Manduca sexta*, maximum power output was recorded at thoracic temperatures (36–42 °C) and wingbeat frequencies (26–32 Hz) matching those observed in free flight; for individual moths, the optimal range was even tighter (Stevenson and Josephson, 1990). Insects appear, therefore, to fly within the narrow range of frequencies which maximises the mechanical performance of their flight muscles.

A reduction in planform area during the upstroke is often observed during the slow flight of vertebrates (e.g. Brown, 1963, for birds; Norberg, 1976, for bats), where it helps to reduce aerodynamic and inertial costs (Spedding, 1992). The design of insect wings, however, prevents large changes in wing planform. The degree of overlap in a wing couple could potentially be varied, but this was not detected for *Manduca sexta*. Bunker (1993) found that if there was a slight trend in butterflies it was for the overlap to *decrease* during the upstroke. The folding in the anojugal region during the *Manduca sexta* upstroke does reduce the planform area, but the maximum extent of this change could only be approximately 4 %, which is the area of the entire flap. The reduction of more than 10 % reported by Wilkin and Williams (1993) for tethered *Manduca sexta* does not occur in free flight. The extreme remotion shown during the upstroke in their study, and the movement of much of the hindwing under the forewing, was not observed during the current study.

There was, however, a very pronounced discrepancy in *Manduca sexta* flight between the durations of the two halfstrokes. The plots of sweep angle *versus* time (Fig. 8) show that the wing motion is not symmetrical: the downstroke was always longer than the upstroke. The ratio between the downstroke and upstroke duration d/u varied between 1.06 and 2.00 with a mean of 1.42. This is in stark contrast to the observed ratios in groups with asynchronous flight muscles: Ellington (1984*b*) found ratios for hovering dipterans and hymenopterans which ranged between 0.91 and 1.13, but with most values between 1.00 and 1.06. In hovering and forward flight, the ratio averaged 0.98 for the hoverfly *Eristalis tenax* (Dudley, 1987) and 1.06 for the bumblebee *Bombus terrestris* (Dudley and Ellington, 1990*a*). There was no relationship between this ratio and flight speed in either study, or in heteropteran forward flight where the values were also close to unity (Betts, 1986). Interestingly, however, the relative duration of the heteropteran downstroke did increase during rising flight.

Butterflies once again display great variability in the shape and duration of their halfstrokes: Bunker (1993) observed d/u values which varied from 0.57 to 2.75, with the majority being greater than 1. Betts and Wootton (1988) reported a tendency for the ratio to be lower in slow flight than in fast flight for *Troides radamantus*, *Papilio rumanzovia* and *Graphium sarpedon*. The aerodynamic significance of asymmetry in the halfstroke durations will be investigated in a companion paper (Willmott and Ellington, 1997*b*).

Wing twist and its changes with forward speed

The data obtained for *Manduca sexta* provide the most

comprehensive picture to date of wing orientation and twisting in a free-flying insect and of how this varies with flight speed. The rotation angle measured here differs from the geometric angle of attack and the angle of incidence which have been determined in previous studies (e.g. Nachtigall, 1966, 1979; Ellington, 1984*b*; Azuma and Watanabe, 1988; Dudley and Ellington, 1990*a*), but the qualitative observations regarding the temporal and spanwise patterns of wing twisting can be compared.

Spanwise variation in wing angle was evident in this and in many other studies (e.g. Jensen, 1956; Norberg, 1972; Nachtigall, 1979; Ellington, 1984*b*; Azuma and Watanabe, 1988). For *Manduca sexta*, especially during slow flight, the rotation angles decreased from wingbase to wingtip during the downstroke, but increased along the wing on the upstroke. During both halfstrokes, therefore, the outer section of the wing was inclined at the lowest angle to the direction of wing motion. The aerodynamic significance of these results requires the orientation of sections relative to the local velocity to be considered (see Willmott and Ellington, 1997*b*), but at a kinematic level they indicate that the wingtip undergoes greater fluctuations in rotation during the course of a wingbeat than does the wingbase. Similar patterns have been measured qualitatively by Ellington (1984*b*) for a range of hovering insects and quantitatively for dragonflies by Azuma and Watanabe (1988) and Zeng *et al.* (1996). In the dragonfly studies, torsion occurred gradually along the length of the wings, in contrast to the more abrupt transition between the two functional sections of the *Manduca sexta* wing couple.

The variation in rotation angle is less pronounced, both spatially and temporally, during the downstroke. The spanwise gradient in angle is very shallow for the *Manduca sexta* wing couple at high forward speeds, and for both the fore- and hindwings of a tethered dragonfly *Sympetrum infuscatum* (Zeng *et al.* 1996). In both these species, the wing orientation is 'set' early in the halfstroke and the angle is then held fairly constant for most of the translational phase. A similar phenomenon has been recorded for both halfstrokes in *Drosophila virilis* (Vogel, 1967) and in a range of hovering insects (Ellington, 1984*b*), but more commonly it appears to be true only for the downstroke (Jensen, 1956; Nachtigall, 1966; Azuma and Watanabe, 1988). In *Manduca sexta*, the pronounced plateau in rotation angle characteristic of the downstroke may be due in part to the longer duration of the downstroke translational phase, but this cannot be a significant factor in the other species. The observed differences in twisting behaviour between the two halfstrokes are more likely to result from the asymmetric resistance to pronatory and supinatory rotation which is inherent in the design of many wings (Wootton, 1993).

The changes in wing twist which accompany increasing flight speed have not been extensively studied. Dudley and Ellington (1990*a*) found that both downstroke and upstroke angles of attack relative to the stroke plane tended to increase with increasing speed in the bumblebee *Bombus terrestris*. Azuma and Watanabe (1988), however, found no such correlation for the dragonfly *Anax parthenope*. The data for *Manduca sexta* show clear changes in wing orientation and twisting. The downstroke angle of rotation increased with flight speed, but the extent of spanwise twisting was reduced. Wing deformation is most pronounced at hovering, while the wing functions as a much more rigid structure in fast forward flight. The greater change in orientation between the two halfstrokes at the lower speeds results in higher angular velocities during stroke reversal.

This paper has described the changes in wing and body kinematics and wing orientation which accompany increases in forward speed. The aerodynamic significance of these changes is considered in Willmott and Ellington (1997*b*), where the results of the kinematic analysis are used in a detailed numerical analysis of the aerodynamic forces and power requirements associated with flight at the different speeds.

Symbols

d/u	Ratio of downstroke to upstroke duration
m	Body mass
n	Wingbeat frequency
R	Wing length
$\hat{S}$	Distance, in wing lengths, from the object to the optical centre of the lens
V	Flight velocity
α_{sp}	Angle of rotation relative to the stroke plane
β	Stroke plane angle
θ	Angle of elevation of the wing with respect to the stroke plane
$\overline{\theta}$	Mean elevation angle
ϕ	Sweep angle of the wing within the stroke plane
ϕ_{min}	Minimum sweep angle (supination)
ϕ_{max}	Maximum sweep angle (pronation)
$\overline{\phi}$	Mean sweep angle
Φ	Stroke amplitude
χ	Body angle
$\overline{\chi}$	Mean body angle

Appendix: error analysis

There are a number of potential sources of error inherent in the analysis procedure for the wingtip kinematics. The first results from the assumption that the wing image is a parallel projection when, in reality, it is a perspective projection (Ellington, 1984*b*). In the current study, the distance, in wing lengths, from the object plane to the optical centre of the lens $\hat{S}$ took values between 27 and 28, corresponding to maximum errors in the positional (sweep and elevation) angles of 2.1 and 2.0 °, respectively (Ellington, 1984*b*). The maximum errors occur in the frame of the maximum projected length; the errors will be lower for the frames at the ends of the wingbeat from which the summary kinematic parameters are calculated.

A second source of error is in the determination of the maximum projected length. Owing to the finite number of

frames per wingbeat, it is unlikely that any frame records the wing exactly perpendicular to the camera axis. The maximum projected lengths were, however, obtained when the wings were slowing down in the second half of the downstroke, giving a higher effective rate of sampling. The maximum projected length should, therefore, be close to the true maximum.

The effects of digitizing error on the positional angles will be most pronounced for frames in which the wing length is close to the maximum projected length. An error of 1 pixel, roughly 1 % of the wing length in these frames, will result in a maximum error of 8 ° (Ellington, 1984*b*). The curves for sweep angle as a function of time (Fig. 8) were relatively smooth in this region, suggesting that the errors were smaller than 8 °. The errors in the upstroke due to ventral flexion are likely to have been more significant, especially as they occurred when the wing was close to the object plane. A 1 % shortening of the projected wing length here may also result in errors of up to 8 °.

In order to quantify the effect of digitizing error on the kinematic parameters, two flight sequences for moth F1 (the middle wingbeats at 0 and 3 m s^{-1}) were digitized three times, with 3 months between the first and last occasions. A full kinematic analysis was carried out for each data set. For the hovering flight sequences, all of the kinematic parameters (including the roll and yaw values) were repeatable to within 1 °, whilst for the higher speed this value was 0.6 °.

The above test examined the effect of any random digitizing errors, but there may also have been systematic errors arising from slight inaccuracies in the estimation of the wingbase position. The effect of moving this position within realistic limits was also quantified. For five wingbeats (M1 at 1 and 3 m s^{-1}, F1 at 0 and 4 m s^{-1}, and F2 at 3 m s^{-1}), the position of the wingbase in the object plane was offset by (+2,+2) and (–2,–2) pixels, thus altering the coordinates of the wingtips which are given relative to the chosen wingbase location. The changes in the summary kinematic parameters were: β, 0.18±0.14 °; Φ, 0.87±0.22 °; $\bar{\phi}$, 0.18±0.08 ° (means ± S.D.). For a more realistic offset of only one pixel in each direction, the changes were approximately halved.

Finally, errors in the wingbeat frequency may result from the finite number of frames per beat and from the loss of every sixth frame on the EktaPro system. The maximum potential error would occur if the true start of the first wingbeat and the end of the third wingbeat had both occurred during missing frames. The error in this case would have been two frames in approximately 120 frames, corresponding to an error of ±0.4 Hz.

The authors are very grateful to Mr P. Goodyer and the EPSRC Instrument Pool for the loan of the EktaPro high-speed video system, to Mr R. Holder for modifying the wind tunnel contraction area, and to Dr J. M. Wakeling, Dr A. L. R. Thomas and Dr R. D. Stevenson for their help and advice concerning the experimental set-up and for many useful discussions. This work was supported by grants from the BBSRC (A.P.W.), the SERC and the Hasselblad Foundation (C.P.E.).

References

AZUMA, A. AND WATANABE, T. (1988). Flight performance of a dragonfly. *J. exp. Biol.* **137**, 221–252.

BAKER, P. S., GEWECKE, M. AND COOTER, R. J. (1981). The natural flight of the migratory locust, *Locusta migratoria* L. III. Wingbeat frequency, flight speed and attitude. *J. comp. Physiol.* A **141**, 233–237.

BETTS, C. R. (1986). The kinematics of Heteroptera in free flight. *J. Zool., Lond.* B **1**, 303–315.

BETTS, C. R. AND WOOTTON, R. J. (1988). Wing shape and flight behaviour in butterflies (Lepidoptera: Papilionoidea and Hesperioidea): a preliminary analysis. *J. exp. Biol.* **138**, 271–288.

BRODSKY, A. K. (1991). Vortex formation in the tethered flight of the Peacock Butterfly *Inachis io* L. (Lepidoptera, Nymphalidae) and some aspects of insect flight evolution. *J. exp. Biol.* **161**, 77–95.

BROWN, R. H. J. (1963). The flight of birds. *Biol. Rev.* **38**, 460–489.

BUNKER, S. J. (1993). Form, flight pattern and performance in butterflies (Lepidoptera: Papilionoidea and Hesperioidea). PhD thesis, University of Exeter.

CHADWICK, L. E. AND EDGERTON, H. E. (1939). *Insects in Flight.* Cambridge, MA: Harvard Film Service.

COOPER, A. J. (1993). Limitations of bumblebee flight performance. PhD thesis, University of Cambridge.

DAVID, C. T. (1978). The relationship between body angle and flight speed in free-flying *Drosophila*. *Physiol. Ent.* **3**, 191–195.

DUDLEY, R. (1987). Forward flight of insects. PhD thesis, University of Cambridge.

DUDLEY, R. (1990). Biomechanics of flight in neotropical butterflies: morphometrics and kinematics. *J. exp. Biol.* **150**, 37–53.

DUDLEY, R. (1992). Aerodynamics of flight. In *Biomechanics – Structures and Systems* (ed. A. A. Biewener), pp. 97–121. Oxford: IRL Press.

DUDLEY, R. AND DEVRIES, P. J. (1990). Flight physiology of migrating *Urania fulgens* (Uraniidae) moths: kinematics and aerodynamics of natural free flight. *J. comp. Physiol.* A **167**, 145–154.

DUDLEY, R. AND ELLINGTON, C. P. (1990*a*). Mechanics of forward flight in bumblebees. I. Kinematics and morphology. *J. exp. Biol.* **148**, 19–52.

DUDLEY, R. AND ELLINGTON, C. P. (1990*b*). Mechanics of forward flight in bumblebees. II. Quasi-steady lift and power requirements. *J. exp. Biol.* **148**, 53–88.

ELLINGTON, C. P. (1984*a*). The aerodynamics of hovering insect flight. II. Morphological parameters. *Phil. Trans. R. Soc. Lond. B* **305**, 17–40.

ELLINGTON, C. P. (1984*b*). The aerodynamics of hovering insect flight. III. Kinematics. *Phil. Trans. R. Soc. Lond. B* **305**, 41–78.

ENNOS, A. R. (1989). The kinematics and aerodynamics of the free flight of some Diptera. *J. exp. Biol.* **142**, 49–85.

GEWECKE, M. (1970). Antennae: another wind-sensitive receptor in locusts. *Nature* **239**, 1263–1264.

GEWECKE, M. (1975). The influence of the air-current sense organs on the flight behaviour of *Locusta migratoria*. *J. comp. Physiol.* **103**, 79–95.

GEWECKE, M., HEINZEL, H.-G. AND PHILIPPEN, J. (1974). Role of antennae of the dragonfly *Orthetrum cancellatum* in flight control. *Nature* **249**, 584–585.

GÖTZ, K. G. (1968). Flight control in *Drosophila* by visual control of motion. *Kybernetik* **4**, 199–208.

HOCKING, B. (1953). The intrinsic range and speed of flight of insects. *Trans. R. ent. Soc. Lond.* **104**, 223–345.

HOLLICK, F. S. J. (1940). The flight of the dipterous fly *Muscina stabulans* Fallén. *Phil. Trans. R. Soc. Lond. B* **230**, 357–390.

JENSEN, M. (1956). Biology and physics of locust flight. III. The aerodynamics of locust flight. *Phil. Trans. R. Soc. Lond. B* **239**, 511–552.

JOSEPHSON, R. K. (1981). Temperature and the mechanical performance of insect muscle. In *Insect Thermoregulation* (ed. B. Heinrich), pp. 19–44. New York: John Wiley & Sons.

KUTSCH, W. AND STEVENSON, P. (1981). Time-correlated flight of juvenile and mature locusts: a comparison between free and tethered animals. *J. Insect Physiol.* **27**, 455–459.

MAGNAN, A. (1934). *La Locomotion chez les Animaux. I. Le Vol des Insectes*. Paris: Hermann et Cie.

MIYAN, J. A. AND EWING, A. R. (1985). Is the 'click' mechanism of dipteran flight an artefact of CCl_4 anaesthesia? *J. exp. Biol.* **116**, 313–322.

NACHTIGALL, W. (1966). Die Kinematik der Schlagflügelbewegungen von Dipteren. Methodische und analytische Grundlagen zur Biophysik des Insektenflugs. *Z. vergl. Physiol.* **52**, 155–211.

NACHTIGALL, W. (1979). Rasche Richtungsänderungen und Torsionen schwingender Fliegenflügel und Hypothesen über zugeordnete instationäre Strömungseffekte. *J. comp. Physiol.* **133**, 351–355.

NACHTIGALL, W. AND WILSON, D. M. (1967). Neuromuscular control of dipteran flight. *J. exp. Biol.* **47**, 77–97.

NORBERG, R. Å. (1972). The pterostigma of insect wings, an inertial regulator of wing pitch. *J. comp. Physiol.* **81**, 9–22.

NORBERG, U. M. (1976). Aerodynamics, kinematics and energetics of horizontal flight in the long-eared bat *Plecotus auritus*. *J. exp. Biol.* **65**, 179–212.

NORBERG, U. M. (1990). *Vertebrate Flight.* Berlin: Springer-Verlag.

RAYNER, J. M. V. (1995). Dynamics of the vortex wakes of flying and swimming vertebrates. In *Biological Fluid Dynamics* (ed. C. P. Ellington and T. J. Pedley). *Symp. Soc. exp. Biol.* **49**, 131–155.

SCHNELL-LARSEN, R. (1934). Der Flug der Insekten. Eine neue Methode zu dessen Erforschung. *Norsk ent. Tidsskr.* **3**, 306–315.

SCHWEMER, J. AND PAULSEN, R. (1973). Three visual pigments in *Deilephila elpenor* (Lepidoptera, Sphingidae). *J. comp. Physiol.* **86**, 215–229.

SOTAVALTA, O. (1947). The flight-tone (wing-stroke frequency) of insects. *Acta ent. fenn.* **4**, 1–117.

SOTAVALTA, O. (1952). The essential factor regulating the wing-stroke frequency of insects in wing mutilation and loading experiments and in experiments at subatmospheric pressure. *Ann. Zool. Soc. Vanamo* **15**, 1–66.

SOTAVALTA, O. (1954). The effect of wing inertia on the wing-stroke frequency of moths, dragonflies and cockroach. *Ann. Zool. Soc. Vanamo* **20**, 93–101.

SPEDDING, G. R. (1992). The aerodynamics of flight. In *Mechanics of Animal Locomotion* (ed. R. McN. Alexander). *Adv. comp. env. Physiol.* **11**, 51–111. Berlin: Springer-Verlag.

STEVENSON, R. D. AND JOSEPHSON, R. K. (1990). Effects of operating frequency and temperature on mechanical power output from moth flight muscle. *J. exp. Biol.* **149**, 61–78.

TOBALSKE, B. W. AND DIAL, K. P. (1996). Flight kinematics of black-billed magpies and pigeons over a wide range of speeds. *J. exp. Biol.* **199**, 263–280.

VOGEL, S. (1967). Flight in *Drosophila.* II. Variations in stroke parameters and wing contour. *J. exp. Biol.* **46**, 383–392.

WAKELING, J. M. AND ELLINGTON, C. P. (1997). Dragonfly flight. II. Velocities, accelerations and kinematics of flapping flight. *J. exp. Biol.* **200**, 557–582.

WEIS-FOGH, T. (1956). Biology and physics of locust flight. II. Flight performance of the Desert Locust (*Schistocerca gregaria*). *Phil. Trans. R. Soc. Lond. B* **239**, 459–510.

WEIS-FOGH, T. (1973). Quick estimates of flight fitness in hovering animals, including novel mechanisms for lift production. *J. exp. Biol.* **59**, 169–230.

WILKIN, P. J. AND WILLIAMS, M. H. (1993). Comparison of the aerodynamic forces on a flying sphingid moth with those predicted by quasi-steady theory. *Physiol. Zool.* **66**, 1015–1044.

WILLMOTT, A. P. AND ELLINGTON, C. P. (1997*a*). Measuring the angle of attack of beating insect wings: robust three-dimensional reconstruction from two-dimensional images. *J. exp. Biol.* **200**, 2693–2704.

WILLMOTT, A. P. AND ELLINGTON, C. P. (1997*b*). The mechanics of flight in the hawkmoth *Manduca sexta*. II. Aerodynamic consequences of kinematic and morphological variation. *J. exp. Biol.* **200**, 2723–2745.

WILLMOTT, A. P., ELLINGTON, C. P. AND THOMAS, A. L. R. (1997). Flow visualization and unsteady aerodynamics in the flight of the hawkmoth *Manduca sexta*. *Phil. Trans. R. Soc. Lond. B* **352**, 303–316.

WOOTTON, R. J. (1993). Leading edge section and asymmetric twisting in the wings of flying butterflies (Insecta, Papilionoidea). *J. exp. Biol.* **180**, 105–117.

ZARNACK, W. (1972). Flugbiophysik der Wanderheuschrecke (*Locusta migratoria* L.). I. Die Bewegungen der Vorderflügel. *J. comp. Physiol.* **78**, 356–395.

ZENG, L., MATSUMOTO, H. AND KAWACHI, K. (1996). A fringe shadow method for measuring flapping angle and torsional angle of a dragonfly wing. *Meas. Sci. Technol.* **7**, 776–781.